AIAA JOURNAL
Vol. 32, No. 8, August 1994

Collisional Quenching Corrections for Laser-Induced Fluorescence Measurements of NO $A^2\Sigma^+$

P. H. Paul,* J. A. Gray,† and J. L. Durant Jr.‡
Sandia National Laboratories, Livermore, California 94551
and
J. W. Thoman Jr.§
Williams College, Williamstown, Massachusetts 01267

Quantitative combustion diagnostics using laser-induced fluorescence require a knowledge of energy transfer and quenching rates at elevated temperatures. Such information is critical both for experimental design and for subsequent reduction of measured signals to measurements of temperature and species concentrations. We present the results of a study of electronic energy transfer in NO $A^2\Sigma^+$. These results are cast in the form of empirical correlations which have been developed to facilitate the practical applications of quenching corrections. The choice of particular functional forms for these correlations is based on a classical collisional model of the process. This model has been calibrated against an extensive set of measured cross sections. Results are presented for a number of species of interest in combustion and aerothermodynamic applications.

Introduction

TO effectively use laser-induced fluorescence (LIF) techniques to study turbulence-chemistry interactions it is essential to be able to accurately correct the measured signal for variations in flowfield properties. Such corrections are practical for single point measurements since the requisite flowfield data can be measured by, for example, laser Raman scattering.[1] For multipoint measurements it is most often not possible to gather the data needed for such corrections on a flow-stopping timescale. Thus to interpret a planar laser-induced fluorescence image as representing a particular flowfield property requires a model for the fluorescence signal to properly select a suitable excitation/detection strategy.

Nitric oxide (NO) is an important combustion-generated pollutant as well as a key tracer species for laser-induced fluorescence flowfield diagnostics.[2,3] A relation for the NO fluorescence signal can be developed by observing the following: when the laser spectral energy flux is sufficiently low, a two-level steady-state approach describes the signal as long as rotational repopulation of the pumped state is reasonably fast[4]; the effects of multiple absorbing transitions are important owing to the relatively strong pressure broadening and dense rotational absorption spectrum exhibited by NO; and, the present experimental evidence suggest that the electronic quenching cross section for NO is independent of rotational level.[5–7] In these limits and for broadband detection, the total fluorescence observed during the laser pulse is written as

$$S_{Lf} = C_{\text{opt}} E_p A / [A + Q(\chi_p, P, T)] \sum_i \{f_{Bi}(T) B_i g_i(\chi_p, P, T)\} \times \chi_{\text{NO}} P / k_B T \quad (1)$$

where the summation is over all transitions i which are excited by the laser. Here C_{opt} is a collection of constants which describe the optical system, E_p is the total laser energy per pulse, and A and B_i are Einstein coefficients. The signal dependence on local thermodynamic conditions is through the Boltzmann population fraction $f_{Bi}(T)$; the line shape function g_i which is a convolution between the laser and absorption spectral profiles; the NO number density $\chi_{\text{NO}} P/k_B T$, and the electronic quenching rate $Q(\chi_p, P, T)$. Here χ_{NO} is the NO mole fraction and the χ_p are the mole fractions of the perturbing species. The total time-integrated signal must also include fluorescence that is collected after the laser pulse, e.g., $S_f \approx S_{Lf}[1 + 1/\tau_L(A + Q)]$ where τ_L is the laser pulse width. Thus, the measured signal has a complicated dependence on local temperature, pressure, and the distribution of collision partners as well as a direct dependence on the number density of the absorbing species.

In most combustion applications the fluorescence signal is collision or quenching dominated, that is, $A << Q$. In this limit and for excitation of an isolated absorption line the field variable dependence in the fluorescence signal has the functional form

$$S_{Lf} \propto f_{Bi}(T)\, g_i(\chi_p, P, T)\, \chi_{\text{NO}} / \langle v_{\text{NO}}(T) \rangle \langle\langle \sigma(\chi_p, T) \rangle\rangle \quad (2)$$

Here we have invoked the definition of the quenching rate $Q = < v_{\text{NO}} ><< \sigma >> P/k_B T$ where $< v_{\text{NO}} > \equiv (8k_B T/\pi m_{\text{NO}})^{1/2}$, and $<< \sigma(\chi_p, T) >>$ is a total electronic quenching cross section. This cross section is given by

$$\langle\langle \sigma(\chi_p, T) \rangle\rangle \equiv \sum_p \chi_p (1 + m_{\text{NO}}/m_p)^{1/2} \langle\langle \sigma_p(T) \rangle\rangle \quad (3)$$

where the summation is over all perturbing species p. The magnitude and temperature dependence of the thermally averaged electronic quenching cross section is perturbing species specific and is defined by $<< \sigma_p >> = < v\sigma_p(v) > / < v >$. Here $\sigma_p(v)$ is the relative velocity dependent cross section obtained by integrating the probability of quenching over the collision impact parameter b. The thermal average is taken over a Boltzmann distribution of collision velocities. Measured values of the NO quenching cross section are strongly species specific and display dramatically different temperature-dependent behavior.[6,8–13]

The line-shape function contains a similar dependence on the collisional bath through the effect of pressure-induced broadening and shift. That is,

$$g_i \equiv \int_{\Delta\nu_l} g_l\{\Delta\nu_l, \nu_l\}\, g_a\{\Delta\nu_{di}(T), \Delta\nu_{ci}(\chi_p, P, T), \delta\nu_{ci}(\chi_p, P, T), \nu_{ai}\}\, d\nu \quad (4)$$

Received April 23, 1993; revision received March 1, 1994; accepted for publication March 28, 1994. Copyright © 1994 by the American Institute of Aeronautics and Astronautics, Inc. All rights reserved.

*Senior Member of the Technical Staff, Combustion Research Facility, MS-9051. Member AIAA.
†Senior Member of the Technical Staff; currently Professor, Department of Chemistry, Room 265 Meyer Hall, Ohio Northern University, Ada, OH 45810.
‡Senior Member of the Technical Staff, Combustion Research Facility, MS-9051.
§Professor, Chemistry Department, 47 Lab Campus Drive.

Here, g_l is the laser spectral profile as a function of the spectral width and center frequency, $\Delta\nu_l$ and ν_l, respectively. The quantity g_a is the absorption line shape as a function of the line center frequency ν_{ai}; the Doppler width is $\Delta\nu_{di} \equiv \nu_{ai}(8\ell n 2k_BT/m_{NO}c^2)^{1/2}$; and the pressure width and shift are $\Delta\nu_{ci} \equiv 2P\Sigma\chi_p\gamma_{pi}(T)$ and $\delta\nu_{ci} \equiv P\Sigma\chi_p\delta_{pi}(T)$, respectively. The summations are over all perturbing species and, like the quenching cross section, the pressure broadening and shift coefficients γ_{pi} and δ_{pi}, respectively, are perturbing species as well as quantum state specific.

When the composition and temperature of the medium is well known, the measured fluorescence signal can be corrected to extract a particular flow variable (e.g., absorbing species mole fraction). However, when fluorescence diagnostics are applied to turbulent reacting flows the gas composition and the temperature are often unknown. In such situations it is desirable to select a particular pump/detect strategy to be able to interpret the signal as having a predominant or at least a determined dependence on field variables. In either case, a knowledge of the species- and temperature-dependent collisional energy transfer cross sections is required. In the following we present a summary of measured NO $A^2\Sigma^+$ ($v' = 0$) electronic quenching rates. A model for the NO quenching process[14] is employed to select an appropriate functional form for the temperature dependence to report the cross sections as analytic correlations. This model is used to extend the measured values to higher temperatures and to describe quenching of NO $A^2\Sigma^+$ ($v' > 0$).

Quenching of NO $A^2\Sigma^+$

A reasonably successful picture for NO quenching is one of electron transfer via an ion-pair intermediate.[14] This harpoon or curve-crossing model takes quenching as proceeding by electron transfer from NO $A^2\Sigma^+$ to the collider M, followed by ion-ion recombination to form an NO $X^2\Pi$-M covalent pair. The initial electron jump occurs at the intersection between the NO_A-M covalent and the NO^+-M^- ionic surfaces (note, we introduce the subscripts to denote the NO neutral electronic states for notational simplicity). This ionic surface in turn makes an inner crossing with the NO_X-M covalent surface on the repulsive wall. The crossings of the ionic surface with the NO_A-M and NO_X-M surfaces can then act as efficient entrance and exit channels for electronic quenching.

The harpoon mechanism can be used to formulate a direct expression for the probability for quenching and thus can yield predictions for the absolute species- and temperature-dependent quenching cross section. At a basic level, the harpoon model predicts a radius r_c for transfer to the ion-pair surface that can be used to estimate a geometric cross section (e.g., $\sigma_g = \pi r_c^2$). The value for this radius is largely determined by the value of the adiabatic electron affinity of the collision partner. At this radius, a Landau-Zener formalism can be used to determine the probability for quenching as a function of the radial velocity, the mixing of the electronic states, and the overlaps of the ion-neutral vibrational wave functions. In this form the harpoon process can be parameterized by three characteristic velocities: the most probable thermal velocity, $v \equiv (2k_BT/\mu)^{1/2}$; a velocity associated with the change in kinetic energy in reaching the outer crossing, $v_E \equiv [2(\varphi^{(c)}(r) - \varphi^{(c)}(r))/\mu]^{1/2}$ where $\varphi^{(c)}(r)$ is the neutral-neutral potential; and v_{LZ}, that radial velocity which gives a $1/e$ probability of not transferring an electron (hence the term curve crossing). The variation in the cross section with temperature is largely determined by the relative magnitudes of these three characteristic velocities.

We have numerically evaluated the full expressions for the quenching cross sections for a combined harpoon and collision-complex mechanism. We find that the harpoon quenching behavior of collision partners can be reduced to the following five general classes.

1) The first class is species having negative ions which are unstable toward autodetachment on a collisional timescale. For example, the affinity of H_2 is nearly -3 eV, which is comparable to the autodetachment width of the negative ion, $H_2^{-2}\Sigma_u^+$. The large negative value for the affinity as well as the very short lifetime of the ion results in a prediction of a negligibly small cross section for quenching by H_2 at thermal energies. The same behavior is predicted for the noble gases, CF_4, SiF_4, and many of the fully saturated hydrocarbons; that is, the entrance channel for electron transfer is energetically inaccessible and the negative ion is unstable toward autodetachment on the collisional timescale. Species in this class are predicted to have negligible quenching cross sections.

2) The second class is species having negative ions that are stable on a collisional timescale but having relatively negative affinities as well as large negative ion polarizabilities, e.g., N_2 and CO with measured affinities of -1.925 and -1.375 eV, respectively. These affinities are sufficiently negative to present an energy barrier to the harpoon mechanism since r_c is on the repulsive wall of the NO_A-M surface. At low temperatures, the cross section then goes as $<<\sigma(T)>> \propto \pi r_c^2 \exp(-v_E^2/v^2)$. At high temperatures, the slope of this function will substantially increase since vibrationally excited collision partners exhibit crossings at larger values of r_c.

When the harpoon process is poorly allowed or energetically inaccessible, secondary quenching mechanisms can be important. For example, NO quenching by CO is predicted to have a near-zero harpoon cross section at room temperature, however, the measured cross section is of order 6 Å^2 at 300 K (Refs. 6 and 12). One plausible explanation is electronic to vibrational energy transfer which would operate for CO (owing to a dipole moment of $0.1D$) but not for N_2 or H_2. A second example is quenching of NO $A^2\Sigma^+(v' = 1)$ by N_2. Electron transfer is strongly allowed for the $\Delta v = 0$ crossings of $NO_A \Rightarrow NO^+$. However, this channel is barely accessible (energetically) for quenching by N_2 at room temperature. The nondiagonal crossing for $NO_A(v' = 1) \Rightarrow NO^+(v' = 0)$ occurs at a larger radius and on a more weakly sloped portion of the covalent potential. The result of including the nondiagonal terms of the electron donor is a prediction of a factor of 2.3 times increase in the cross section for quenching of $NO_A(v' = 1)$ over that for $NO_A(v' = 0)$ by N_2 at 300 K.

3) The third class is species with moderately negative affinities and strongly attractive covalent potentials, e.g., H_2O and CO_2. A strongly attractive covalent surface can lead to the formation of a centripetal barrier (located at a radius r_b). Collisions with particular impact parameter and relative velocity pairs can cross this barrier leading to the formation of a relatively long-lived collision complex. At low temperatures the radius for this process may be such that $r_b > r_c$, whereas at high temperatures, hence large relative velocities, the converse may be true. Such is the case for quenching by H_2O and CO_2. For low temperatures the value of the cross section is dominated by collisional capture leading to a power-law decrease in the cross section with increasing temperature. At high temperatures the crossing is sufficiently attractive that the cross section is constant with temperature. A similar behavior is found for quenching by SO_2 which has a large positive affinity and dipole moment.

4) The next class is species with moderately positive affinities and reasonably strong neutral-negative ion vibrational overlaps, e.g., NO, O_2, OH, H, and O. Here, for temperatures in excess of 300 K, the strongly allowed crossing is at a radius such that $r_b < r_c$. Thus the cross section is functionally constant with temperature. As mentioned earlier, the $\Delta v = 0$ crossings of $NO_A \Rightarrow NO^+$ are strongly allowed owing to the Rydberg nature of NO $A^2\Sigma^+$. When such crossing are energetically accessible, the model predicts a very weak dependence of the cross section on the NO $A^2\Sigma^+$ vibrational level.

5) The last class is species with large positive affinities and/or weakly allowed ground state neutral-negative ion vibrational overlaps, e.g., NO_2 and a number of the halocarbons. Here, crossings occur at such a large radius that there is a poor overlap of the electronic wave functions. Electron transfer at the large radii crossings, which correspond to the low vibrational levels in the collision partner, is only probable for small radial velocities, whereas crossings that correspond to higher vibrational states in the collision partner, which are at smaller radii, provide a strongly allowed channel for electron transfer. Thus the low temperature cross section is expected to fall roughly as T^{-1} whereas the high-temperature cross section is expected to be relatively constant. For quenching of NO $A^2\Sigma^+$ by NO_2 the harpoon geometric cross section is 344 Å^2; a geometric cross section with allowance for the neutral-negative ion vi-

Table 1 Fitting coefficients for quenching of NO $A^2\Sigma^+$[a]

M	Class	c_0, Å^2	c_1	c_2	c_3	c_4	T[b], K	Note
Nobles	1	0.0					300–1900	c
CH_4	1	0.0					300, 1450	c
C_2H_6	1	0.0					300, 813	c
CF_4	1	0.0					300	c
SiF_4	1	0.0					300	c
H_2	1	0.0					300–1900	c
N_2	2	0.0	0.88	4.8	3.1	16.0	300–4500	$v'=0$[d]
	2	0.0	0.88	4.9	48.0	32.0	300–4500	$v'=0$[e]
	2	0.0	1.3	4.4	54.0	28.0	300, 1900	$v'=1$[e]
CO	2	5.9	5.3	7.0	22.1	14.0	300–2300	$v'=0$[d]
H_2O	3	28.2	3.39	0.15	2.95		300–2300	
CO_2	3	54.2	0.95	3.24	0.18		300–2300	
N_2O	3	59.0	0.99	3.98	0.16		300, 1450, 2300	
SO_2	3	52.0	1.68	0.11	3.01		300	
NO	4	43.0					300–4500	c
O_2	4	25.1					300–2300	c
O	4	32.0					1600	c
H	4	12.0					1600	c
OH	4	82.0					1600, 2300	c
NH	4	58.0					NA	c,d
CH	4	101.0					NA	c,d
NO_2	5	82.0	9.0	0.54			300, 1450, 1900	

[a]Fits for $v'=0$ and 300–4500 K except as noted; $T_r \equiv 300$ K.
[b]Temperature range for verification to experimental data.
[c]Predicted $\ll \sigma \gg \neq f(v')$ for $v' \leq 3$ in NO_A.
[d]Fit to full model predicted values.
[e]Fit to measured values.

brational overlaps gives a value of 42 Å^2, whereas the measured values range between 46 Å^2 (Ref. 13) and 90 Å^2 (Ref. 12).

This classification of the species- and temperature-dependent quenching behavior has been verified by comparison to experimentally measured cross sections. To a reasonable level the model is successful at predicting the absolute magnitudes of the cross sections when the harpoon mechanism is the dominant channel for electronic energy transfer. This appears to be the case for most of the collision partners that have been experimentally studied to date with a particular exception: species having an excited electronic energy level at or slightly below that of NO $A^2\Sigma^+$. This last class of collision partners may exhibit near-resonant electronic energy exchange. Such behavior has been observed for quenching of NO $A^2\Sigma^+$ by C_2H_2, C_2H_4, and NH_3 (Ref. 16), as well as benzene, toluene, and CH_3I (Ref. 13).

We have considered the asymptotic behavior of the thermally averaged quenching cross section for the combined harpoon/collision-complex mechanism.[14] For the classes just described, this analysis suggests the following functional forms:

Class 1

$$\langle\langle \sigma_p \rangle\rangle \approx 0.0 \tag{5a}$$

Class 2

$$\langle\langle \sigma_p \rangle\rangle \approx c_0 + c_1 \exp(-c_2 T_r/T) + c_3 \exp(-c_4 T_r/T) \tag{5b}$$

Class 3

$$\langle\langle \sigma_p \rangle\rangle \approx c_0 \{(1+\eta)\exp(-\eta) + c_1 \eta^{1/3} \gamma(5/3, \eta)\} \tag{5c}$$

$$\eta \equiv c_2 (T_r/T) + c_3 (T_r/T)^2$$

Class 4

$$\langle\langle \sigma_p \rangle\rangle \approx c_0 \tag{5d}$$

Class 5

$$\langle\langle \sigma_p \rangle\rangle \approx c_0 + c_1 (T_r/T)^{c_2} \tag{5e}$$

In Eq. (5c), $\gamma(a,x)$ is the incomplete gamma function.[15] The constants c_i in Eqs. (5) have been determined by comparison to measurements and to numerical predictions of the full model. These constants along with the applicable temperature range are given in Table 1. These data and the results of a similar study on electronic quenching of OH $A^2\Sigma^+$ are also made available as a database which includes a Fortran routine to evaluate the corresponding functions.[16] Comparison of the model predictions, measured data, and these correlations are shown for quenching by N_2 in Fig. 1, CO and CO_2 in Fig. 2, and H_2O in Fig. 3.

Heard et al.[17] measured the total fluorescence decay rates from NO $A^2\Sigma^+$ in a 30-Torr premixed CH_4-air flame. Using a radiative decay rate of 4.55 μs^{-1} and measured temperatures of 1190 and 1680 K, they found total NO quenching rates of 25.5 and 28.5 μs^{-1} at downstream positions of 0.85 and 1.73 cm, respectively. Using calculated species profiles and estimates for the high-temperature quenching cross sections they predicted values of 23.1 and 29.7 μs^{-1}, respectively. Using a radiative rate of 4.85 μs^{-1} (Ref. 11), the measured quenching rates change to 25.1 and 28.1 μs^{-1}, respectively. Using the correlations given in Table 1, we find values of 25.4 and 27.3 μs^{-1}, respectively. Both sets of predictions are within 10% of the measured values. Compared to the species specific values cited by Heard et al.,[17] the values here (Table 1) provide faster rates for N_2, O_2, and H_2O and a much slower rate for CO_2. For the 1680 K case the prediction increases when the rates for quenching by H and OH are included (2.1 and 1.45 μs^{-1}, respectively) to a value of 30.85 μs^{-1}.

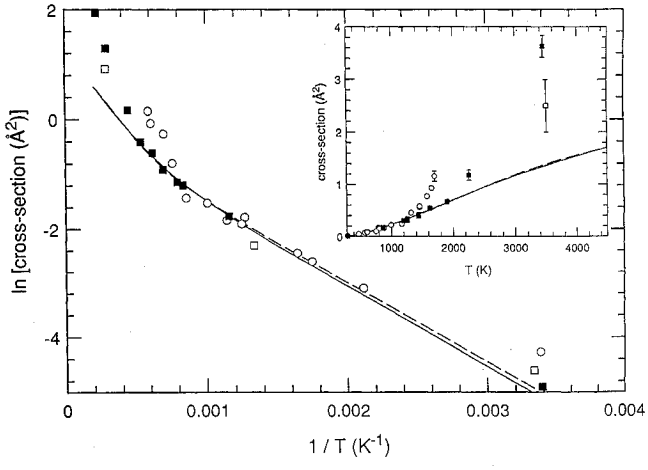

Fig. 1 Cross section for quenching of NO $A^2\Sigma^+(v'=0)$ by N_2 shown as an Arrhenius plot: dashed line, full model prediction for collisions with a thermal distribution of N_2 vibrational states; solid line, correlation to model; measured values, ■Ref. 11, ○ Ref. 6, and □ Ref. 9. The inset figure shows the same predictions and measured data plotted in linear form.

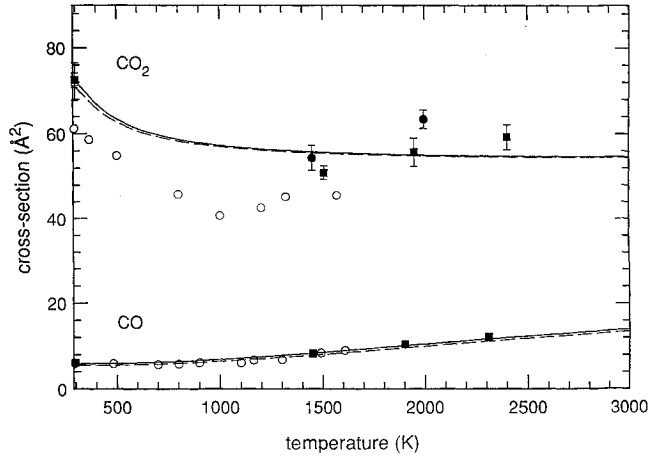

Fig. 2 Cross section for quenching of NO $A^2\Sigma^+(v'=0)$ by CO and CO_2: dashed lines, full model prediction; solid lines, correlation to model; measured values, ■Ref. 12, ● Ref. 10, ○ Ref. 6, and □ Ref. 13.

Schwarzwald et al.[18] performed a series of NO quenching measurements in atmospheric pressure flames using picosecond excitation techniques. They studied premixed conditions including a fuel-lean ($\varphi \approx 0.5$) CH_4-N_2O flame at near 2100 K and a fuel-rich ($\varphi \approx 1.92$) CH_4-air flame at near 1900 K, both doped with a trace of NO. They determined collisional lifetimes (e.g., $\tau = 1/Q$) of 1.7 $\pm$ 0.3 and 1.5 $\pm$ 0.3 ns for these conditions, respectively. Assuming an equilibrium collisional bath (at the reported temperatures) and using the correlations given in Table 1 we estimate collisional lifetimes of 1.67 and 1.58 ns, respectively, which are in good agreement with the measurements.

Implications for NO Laser-Induced Fluorescence Measurements

We now consider the effect of species-specific quenching on the NO fluorescence signal. The LIF signal is taken to be given by Eq. (2), which is appropriate for linear excitation of single isolated transitions and collision dominated fluorescence. In this limit the LIF signal is a function of three field variables: T, χ_{NO}, and the collisional bath. When the total cross section varies weakly or as a known power law with temperature it may be possible to select a rotational transition that provides a nearly temperature-independent signal over some finite temperature range; hence, the signal represents a measure of the absorbing species mole fraction. This particular technique has been used for planar laser-induced fluorescence (PLIF) imaging of OH $A^2\Sigma^+$ in atmospheric pressure nonpremixed flames.[19] Alternatively, by seeding the flow with NO the LIF signal can be used as a measure of temperature with the assumptions that NO is a conserved scalar and that a simple power-law temperature dependence describes the total quenching cross

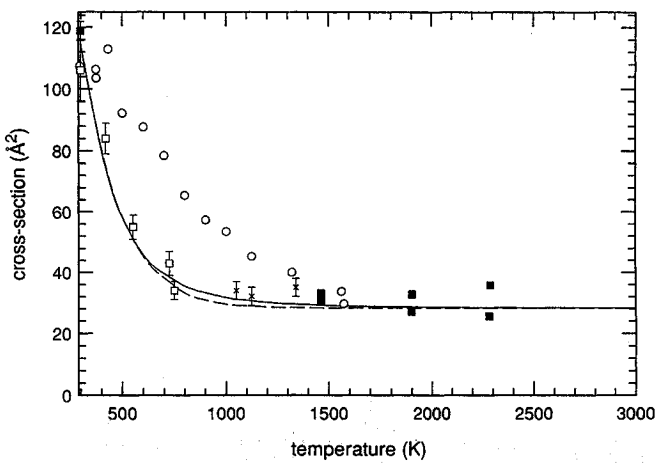

Fig. 3 Cross section for quenching of NO $A^2\Sigma^+(v'=0)$ by H_2O. Dashed line, model prediction; solid line, correlation to model; measured values, ■Ref. 12, ○ Ref. 6, □ Ref. 9, and × Ref. 8.

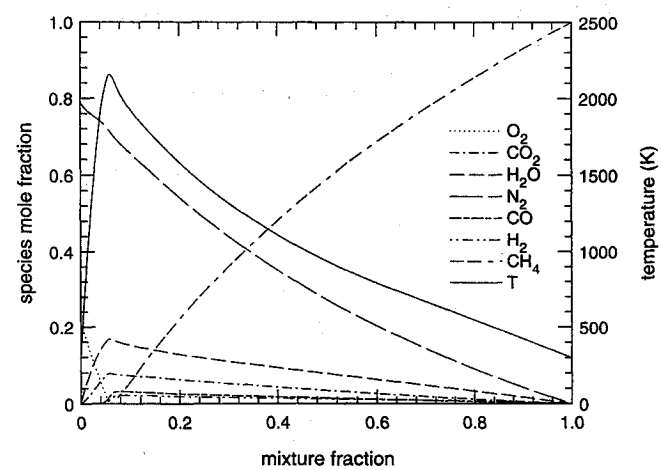

Fig. 4 Distribution of major species and temperature in a strained laminar CH_4-air flame (strain rate of 50 s^{-1}) as a function of mixture fraction.

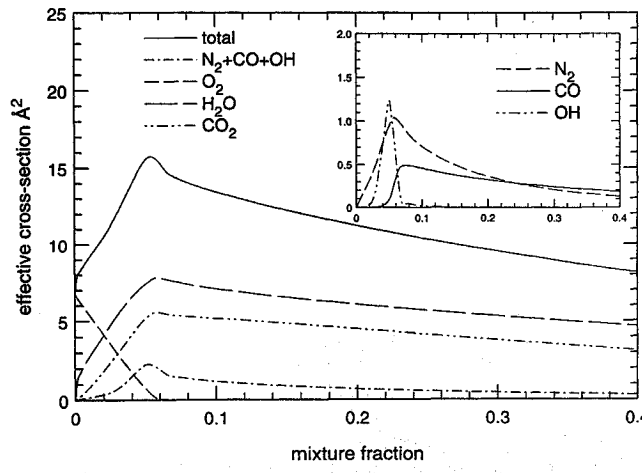

Fig. 5 Predicted species specific and total effective cross sections for quenching of NO $A^2\Sigma^+(v'=0)$ for conditions shown in Fig. 4 (note change of horizontal scale). The inset figure shows the contributions of the minor quenchers.

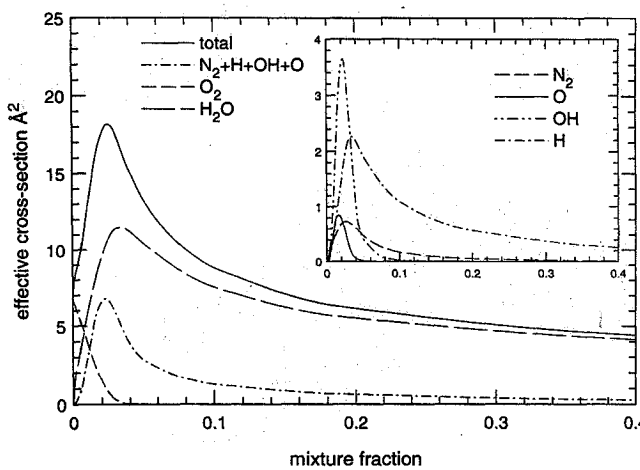

Fig. 6 Predicted species specific and total effective cross sections for quenching of NO $A^2\Sigma^+(v'=0)$ for conditions of a strained laminar H_2-air flame, strain rate of 1000 s^{-1}. The inset figure shows the contributions of the minor quenchers.

section.[3] Such limiting cases can provide unique opportunities to use single-laser LIF and PLIF diagnostics to make measurements in turbulent reacting flows. In the following we investigate the variation in the collsional quenching and line broadening under reacting flow conditions.

First we consider a nonpremixed reacting flow, specifically, the case of a strained laminar flame. Results are presented as a function of mixture fraction f, which is a progress variable defined as zero in pure oxidizer and unit in pure fuel. These calculations are parameterized by a strain parameter, which is defined for a cylinder of radius r in a crossflow of velocity U by $a = 2U/r$. The variation of species and temperature for a strained laminar CH_4-air flame is shown in Fig. 4. Figure 5 shows the corresponding variation in the effective species-specific and total quenching cross sections. Here, the effective cross section is simply defined as the relative mass weighted cross section; $\sigma_{ep} \equiv (1 + m_{NO}/m_p)^{1/2} << \sigma_p(T) >>$. These values were obtained using the correlation parameters given in Table 1. On the oxidizer side of the flame ($f < 0.0607$) one observes a definite change in the slope in the total cross section. This results from the decreased contribution of quenching by O_2 and the strong increase in the contribution from H_2O for temperatures below 1000 K. Quenching by OH appears to be the third strongest term in the region of the flame, whereas quenching on the rich side is dominated by the contributions of CO_2 and H_2O. The quenching goes to zero in the pure fuel. A sim-

ilar result for a strained laminar H_2-air flame is shown in Fig. 6. On the fuel lean side quenching by OH can contribute as much as 30% to the total cross section. On the fuel rich side quenching by H can contribute as much as 20% to the total cross section.

For both the CH_4-air and H_2-air results we find that the total effective cross section follows roughly a $T^{0.6}$ dependence on the lean side, but shows a $T^{1.2}$ to $T^{1.6}$ dependence on the rich side of the flame. Because the total NO quenching cross section displays a strong positive power-law dependence, a direct measurement of the mole fraction would require pumping of a very high rotational level. However, excitation of high rotational levels would result in a severe penalty in signal and may be subject to strong interference from adjacent transitions. In using a transition closer to the peak of the rotational distribution, a more appropriate interpretation of the signal would be as an indicator of NO density (e.g., $S_f \propto \rho_{NO} = \chi_{NO} P/k_B T$).

Figure 7 shows the effective cross sections for quenching of NO $A^2\Sigma^+$ for the conditions of a laminar premixed C_2H_6-N_2-O_2 flame ($\varphi = 0.8$ and $N_2/O_2 = 3.1$) plotted as a function of distance downstream from the burner surface. In this flow, once the reaction is reasonably complete (say, for $x > 0.1$ cm) the collisional bath remains relatively constant and the temperature decreases with downstream distance. Thus, effective cross sections are relatively constant because the cross sections are nearly temperature independent (for temperatures over 1000 K). Whereas in the flame zone, however, the large variation in temperature and composition result in very steep spatial gradients in the cross section, hence in the weighting of the LIF signal (e.g., the tempeature and collsional bath dependence).

Only a limited data base for pressure broadening and shift in NO $A \leftarrow X$ is available.[20,21] These measurements suggest that the respective broadening and shift coefficients are weakly dependent on rotational level and collision partner. Analysis of these data and the more recent measurements of broadening of NO $A \leftarrow X$ by He, N_2, and CO_2 (Ref. 22) suggest that the broadening and shift of NO $A \leftarrow X$ (with the likely exception of that by He) follows a simple Foley-Lindholm behavior.[23] Thus, for all perturbers we use the temperature-dependent relations for 2γ and δ for N_2 reported by Chang et al.[21] For each perturber, the magnitude of these parameters is scaled by the product of a reduced-mass weighting and a gas-kinetic cross section. For example,

$$\Delta\nu_c \equiv \Delta\nu_c(N_2, T) \sum_p \chi_p \sigma_{pGK} (1 + m_{NO}/m_p)^{1/2} / \sigma_{N_2GK} (1 + m_{NO}/m_{N_2})^{1/2} \quad (6)$$

Here values for the gas-kinetic cross sections σ_{GK} were obtained from the correlations given by Cambi et al.[24]

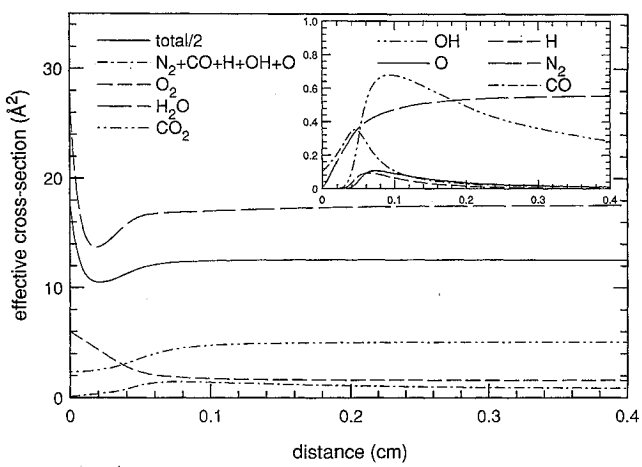

Fig. 7 Predicted species specific and total effective cross sections for quenching of NO $A^2\Sigma^+(v' = 0)$ for conditions of premixed laminar C_2H_6-N_2-O_2 flame ($\varphi = 0.8$, $N_2/O_2 = 3.1$) as a function of distance from the burner surface. The inset figure shows the contributions of the minor quenchers.

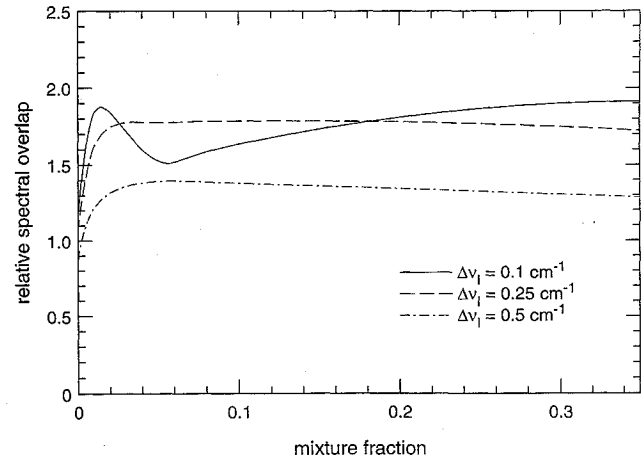

Fig. 8 Variation in the laser-absorption line shape overlap integral for conditions shown in Fig. 4.

Figure 8 shows the spectral convolution integral [Eq. (4)] for an isolated absorption line and for the strained flame conditions of Fig. 4. The laser line shape is taken to be a Gaussian and assumed to be tuned to the absorption maximum for a trace of NO in 1 atm of N_2. The absorption line shape is taken to be a generalized Voigt function which includes the effects of Doppler and collisional broadening and of collision-induced shift. For a relatively narrow laser line width of 0.1 cm^{-1}, a strong variation is found due to both broadening and shift which also indicates that the field dependence must also be a strong function of the exact tuning of the laser. This sensitivity is noticeably reduced for laser line widths greater than 0.2 cm^{-1} except for fuel-lean conditions. Because the reduced-mass weighted cross sections for all of the major collision partners are nearly equal, this result is weakly dependent on the collisional bath. The primary dependence is that on temperature in the collisional broadening and shift. Here, we have considered the effect on an isolated absorption line. However, the NO absorption spectrum is quite dense, thus the effects of adjacent spectral transitions cannot be properly neglected in evaluating the field dependence in the absorption overlap integral.

From the model we can make several additional observations: First, quenching of NO $A^2\Sigma^+$ should proceed with a strong tendency to produce vibrationally excited NO $X^2\Pi$. Thus, little or no recycling of the population would be expected on the timescale of a typical laser pulse given the relatively slow vibrational relaxation rates in the ground electronic state.[25] Second, the long range anisotropy of the attractive potential surface appears to play a fundamental role in rotational-level-dependent quenching.[26] This has been observed in quenching and vibrational relaxation of OH $A^2\Sigma^+$ for low to moderate rotational quantum numbers and for the temperature range of 300–1200 K. A similar effect should operate in quenching of NO $A^2\Sigma^+$ but may only be found for low rotational quantum numbers and temperatures less than 300 K. In LIF temperature measurements rotational-level-dependent quenching represents a significant systematic error.[27] For LIF of NO this is not an issue for combustion measurements, but it will be important when NO is used for measurements in highly expanded supersonic flows (e.g., in shock tunnels[28]). Finally, the cross section and temperature dependence for quenching of NO $A^2\Sigma^+$ by species other than those of class 4 will be a strong function of the vibrational distribution in the collision partner. This is an important issue for hypersonic testing in shock tunnels where the large amount of NO produced in the tunnel provides a convenient diagnostic tracer; however, the flow is often in vibrational nonequilibrium. For example, for quenching of NO $A^2\Sigma^+(v' = 0)$ by N_2, the model predicts a cross section of < 0.01 $Å^2$ at 300 K in equilibrium. However, for a condition of two-temperature translational-vibrational nonequilibrium, the model predicts a value of 0.6 $Å^2$ for a translational temperature of 300 K and an N_2 vibrational temperature of 1200 K.

Conclusions

We have considered a harpoon mechanism to describe quenching of NO $A^2\Sigma^+$ by a wide variety of collision partners. When combined with the action of a collision-complex the model is found to be reasonably successful in predicting both the magnitude and the temperature dependence of the quenching cross section. The harpoon quenching behavior has been divided into five categories, roughly according to the value of the adiabatic electron affinity of the collision partner. A sixth category was identified as composed of those collision partners that exhibit a larger cross section for resonant energy transfer than for harpoon quenching. Based on asymptotic solutions for the combined harpoon and collision-complex mechanisms, a corresponding set of five generic expressions for the temperature-dependent quenching cross section were proposed. Curve-fit coefficients were provided for a number of species which are of interest in combustion and aerothermodynamic applications.

These data were employed to consider the effect of temperature- and collision-partner-dependent quenching on laser-induced fluorescence of NO in premixed and nonpremixed reacting flows. At high temperatures the direct temperature dependence was found to be quite weak, but the collision-partner dependence was seen as very strong, in particular due to the action of atomic and diatomic radicals. The effect of collisional broadening and shift of the NO absorption lines was also found to introduce a noticeable variation in the fluorescence signal with temperature, whereas a weak dependence on the collisional bath was observed. Measurements suggest that there is little or no rotational-level dependence on the NO $A^2\Sigma^+$ quenching cross section for temperatures over 300 K. However, it is quite likely that such a dependence will be found for low rotational levels at lower temperatures. The distribution of population in the vibrational state of the collision partner was found to strongly effect the NO $A^2\Sigma^+$ quenching cross section. Finally, the harpoon mechanism suggests that quenching of NO $A^2\Sigma^+$ will proceed with a disposition to produce vibrationally excited NO $X^2\Pi$.

Acknowledgments

This research was supported by the U.S. Department of Energy, Office of Basic Energy Sciences, Chemical Sciences Division. The fourth author acknowledges the support of Associated Western Universities for an AWU-DOE faculty sabbatical fellowship. The laminar diffusion flame calculations were provided by J. Y. Chen, University of California, Berkeley, who is gratefully acknowledged. The premixed flame calculations were provided by John Reisel of Purdue University, who is gratefully acknowledged.

References

[1]Dibble, R. W., Masri, A. R., and Bilger, R. W., "The Spontaneous Raman Scattering Technique Applied to Nonpremixed Flames of Methane," *Combustion and Flame*, Vol. 67, 1987, pp. 189–206: Pitz, R. W., Wehrmeyer, J. A., Bowling, J. M., and Cheng, T. S., "Single Pulse Vibrational Raman Scattering by a Broadband KrF Excimer Laser in a Hydrogen-Air Flame," *Applied Optics*, Vol. 29, 1990, pp. 2325–2332.

[2]Paul, P. H., Lee, M. P., and Hanson, R. K., "Molecular Velocity Imaging of Supersonic Flows Using Pulsed Planar Laser-Induced Fluorescence of NO," *Optics Letters*, Vol. 14, 1989, pp. 417–419: McMillin, B. K., Lee, M. P., and Hanson, R. K., "Planar Laser-Induced Fluorescence Imaging of Shock-Tube Flows with Vibrational Nonequilibrium," *AIAA Journal*, Vol. 30, 1991, pp. 436–443.

[3]Seitzman, J. M., Kychakoff, G., and Hanson, R. K., "Instantaneous Temperature Field Measurements Using Planar Laser-Induced Fluorescence," *Optics Letters*, Vol. 10, 1985, pp. 439–441.

[4]Zizak, G., Lanauze, J. A., and Winefordner, J. D., "An Experimental Study of the Excited State Rotational Population of OH in Flames Using Laser Induced Fluorescence," *Combustion and Flame*, Vol. 65, 1986, pp. 203–214.

[5]Zacharias, H., Halpern, J. B., and Welge, K. H., "Two-Photon Excitation of NO($A^2\Sigma^+$; $v' = 0, 1, 2$) and Radiation Lifetime and Quenching Measurements," *Chemical Physics Letters*, Vol. 43, 1976, pp. 41–44.

[6]Drake, M. C., and Ratcliffe, J. W., "High Temperature Quenching Cross Sections for Nitric Oxide Laser-Induced Fluorescence Measurements," *Journal of Chemical Physics*, Vol. 98, 1993, pp. 3850–3865.

[7]MacDermid, I. S., and Laudenslanger J. B., "Radiative Lifetimes and Electronic Quenching Rate Constants for Single-Photon-Excited Rotational Levels of NO ($A^2\Sigma^+$, $v' = 0$)," *Journal of Quantitative Spectroscopy and Radiative Transfer*, Vol. 27, 1982, pp. 483–492.

[8]Cattolica, R. J., Mataga, T. G., and Cavolowsky, J. A., "Electronic Quenching and Vibrational Relaxation of NO $A^2\Sigma^+$ ($v' = 0$ and $v' = 1$)," *Journal of Quantitative Spectroscopy and Radiative Transfer*, Vol. 42, 1989, pp. 499–508.

[9]Raiche, G. A., and Crosley, D. R., "Temperature Dependent Quenching of the $A^2\Sigma^+$ and $B^2\Pi$ States of NO," *Journal of Chemical Physics*, Vol. 92, 1990, pp. 5211–5218: Meier, U. E., Raiche, G. A., Crosley, D. R., Smith, G. P., and Eckstrom, D. J., "Laser-Induced Fluorescence Decay Lifetimes of Shock-Heated NO ($A^2\Sigma^+$)," *Applied Physics B*, Vol. 53, 1991, pp. 138–141.

[10]Gray, J. A., Paul, P. H., and Durant, J. L., "Electronic Quenching Rates for NO($A^2\Sigma^+$) Measured in a Shock Tube," *Chemical Physics Letters*, Vol. 190, 1992, pp. 266–270.

[11]Thoman, J. W., Jr., Gray, J. A., Durant, J. L., Jr., and Paul, P. H., "Collisional Electronic Quenching of NO $A^2\Sigma^+$ by N_2 from 300 to 4500 K," *Journal of Chemical Physics* , Vol. 97, 1992, pp. 8156–8163.

[12]Paul, P. H., Gray, J. A., Durant, J. L., Jr., and Thoman, J. W., Jr., "Collisional Electronic Quenching of NO $A^2\Sigma^+$ by H_2O, O_2, CO, CO_2, NO, NO_2, N_2O, N_2, CH_4, H^2, He and Ar," *Journal of Chemical Physics*, (submitted for publication, 1994).

[13]Asscher M., and Haas Y., "The Quenching Mechanism of Electronically Excited Rydberg States of Nitric Oxide," *Journal of Chemical Physics*, Vol. 76, 1982, pp. 2115–2126: Haas, Y., and Greenblatt, G. D., "A Charge Transfer Model for Quenching of Electronically Excited Nitric Oxide, Electron Affinity of the Quenchers," *Journal of Physical Chemistry*, Vol. 90, 1986, pp. 513–517: Greenblatt, G. D., and Ravishankara, A. R., "Collisional Quenching of NO(A, $v' = 0$) by Various Gases," *Chemical Physics Letters*, Vol. 136, 1987, pp. 501–505.

[14]Paul, P. H., Gray, J. A., Durant, J. L., Jr., and Thoman, J. W., Jr., "A Model for Collisional Electronic Quenching of NO $A^2\Sigma^+$," *Applied Physics B*, Vol. 57, 1993, pp. 249–259.

[15]Abramowitz, M., and Stegun, I. A., *Handbook of Mathematical Functions*, 1st ed., Dover, New York, 1972, Eq. 6.5.2, p. 260.

[16]Paul, P. H., Carter, C. D., Gray, J. A., Durant, J. L., Jr., and Thoman, J. W., Jr., "Correlations for the Temperature Dependent Electronic Quenching Cross Sections of NO $A^2\Sigma^+$ and OH $A^2\Sigma^+$," Sandia National Laboratories Rept., Sandia National Lab., Livermore, CA, 1994 (to be published).

[17]Heard, D. E., Jefferies, J. B., and Crosley, D. R., "Collisional Quenching of $A^2\Sigma^+$ NO and $A^2\Delta$ CH in Low Pressure Flames," *Chemical Physics Letters*, Vol. 178, 1991, pp. 533–537: Heard, D. E., Jefferies, J. B., Smith, G. P., and Crosley, D. R., "LIF Measurements in Methane/Air Flames of Radicals Important in Prompt-NO formation," *Combustion and Flame*, Vol. 88, 1992, pp. 137–147.

[18]Schwarzwald, R., Monkhouse, P., and Wolfrum, J., "Fluorescence Lifetimes for Nitric Oxide in Atmospheric Pressure Flames Using Picosecond Excitation," *Chemical Physics Letters*, Vol. 158, 1989, pp. 60–64.

[19]Allen, M. G., and Hanson, R. K., "Digital Imaging of Species Concentration in Spray Flames," *21st Symposium (International) on Combustion*, Combustion Inst., Pittsburgh, PA, 1986, pp. 1755–1761.

[20]Dodge, R. P., Dusek, J., and Zabelinski, M. F., "Line Broadening and Oscillator Strength Measurements for the Nitric Oxide $\gamma(0, 0)$ Band," *Journal of Quantitative Spectroscopy and Radiative Transfer*, Vol. 24, 1980, pp. 237–249.

[21]Chang, A. Y., Dirosa, M. D., and Hanson, R. K., "Temperature Dependence of Collisional Broadening and Shift in the NO $A \leftarrow X$ (0, 0) Band in the Presence of Argon and Nitrogen," *Journal of Quantitative Spectroscopy and Radiative Transfer*, Vol. 47, 1992, pp. 375–390.

[22]Danehy, P. M., Friedman-Hill, E. J., Lucht, R. P., and Farrow, R. L., "The Effects of Collisional Quenching on Degenerate Four-Wave Mixing," *Applied Physics B*, Vol. 57, 1993, pp. 243–248.

[23]Townes, C. H., and Schawlow, A. L., *Microwave Spectroscopy*, 1st ed., Dover, New York, 1975, pp. 347–361.

[24]Cambi, R., Cappelletti, D., Liuti, G., and Pirani, F., "Generalized Correlations in Terms of Polarizability for Van Der Waals Interaction Potential Parameter Calculations," *Journal of Chemical Physics*, Vol. 95, 1991, pp. 1852–1861.

[25]Stephenson, J. C., "Vibrational Relaxation of NO $X^2\Pi(v = 1)$ in the Temperature Range 100–300 K," *Journal of Chemical Physics*, Vol. 60, 1974, pp. 4289–4294.

[26]Copeland, R. A., Wise, M. I., and Crosley, D. R., "Vibrational Energy Transfer and Quenching of OH($A^2\Sigma^+$, $v' = 1$)," *Journal of Physical Chemistry*, Vol. 92, 1988, pp. 5710–5715.

[27]Paul, P. H., Meier, U. E., and Hanson, R. K., "Single-Shot, Multiple-Camera Planar Laser-Induced Fluorescence Imaging in Gaseous Flows," AIAA Paper 91-0459, Jan. 1991.

[28]Palmer, J. L., McMillin, B. K., and Hanson, R. K., "Planar Laser-Induced Fluorescence Imaging of Velocity and Temperature in Shock Tunnel Free Jet Flow," AIAA Paper 92-0762, Jan. 1992.